

## Supporting Information

### **In-Depth Analysis of Excitation Dynamics in Dye-Sensitized Upconversion Core and Core/Active Shell Nanoparticles.**

*Sergey Alyatkin<sup>1\*</sup>, Elena Ureña-Horno<sup>2</sup>, Bigeng Chen<sup>2</sup>, Otto L. Muskens<sup>2</sup>, Antonios G. Kanaras<sup>2</sup> and Pavlos G. Lagoudakis<sup>1,2\*</sup>*

<sup>1</sup> Skolkovo Institute of Science and Technology, Nobel St, 3, Moscow, 121205, Russia

<sup>2</sup> Department of Physics and Astronomy, University of Southampton, Southampton, SO17 1BJ, UK

\* e-mail: s.alyatkin@skoltech.ru; p.lagoudakis@skoltech.ru

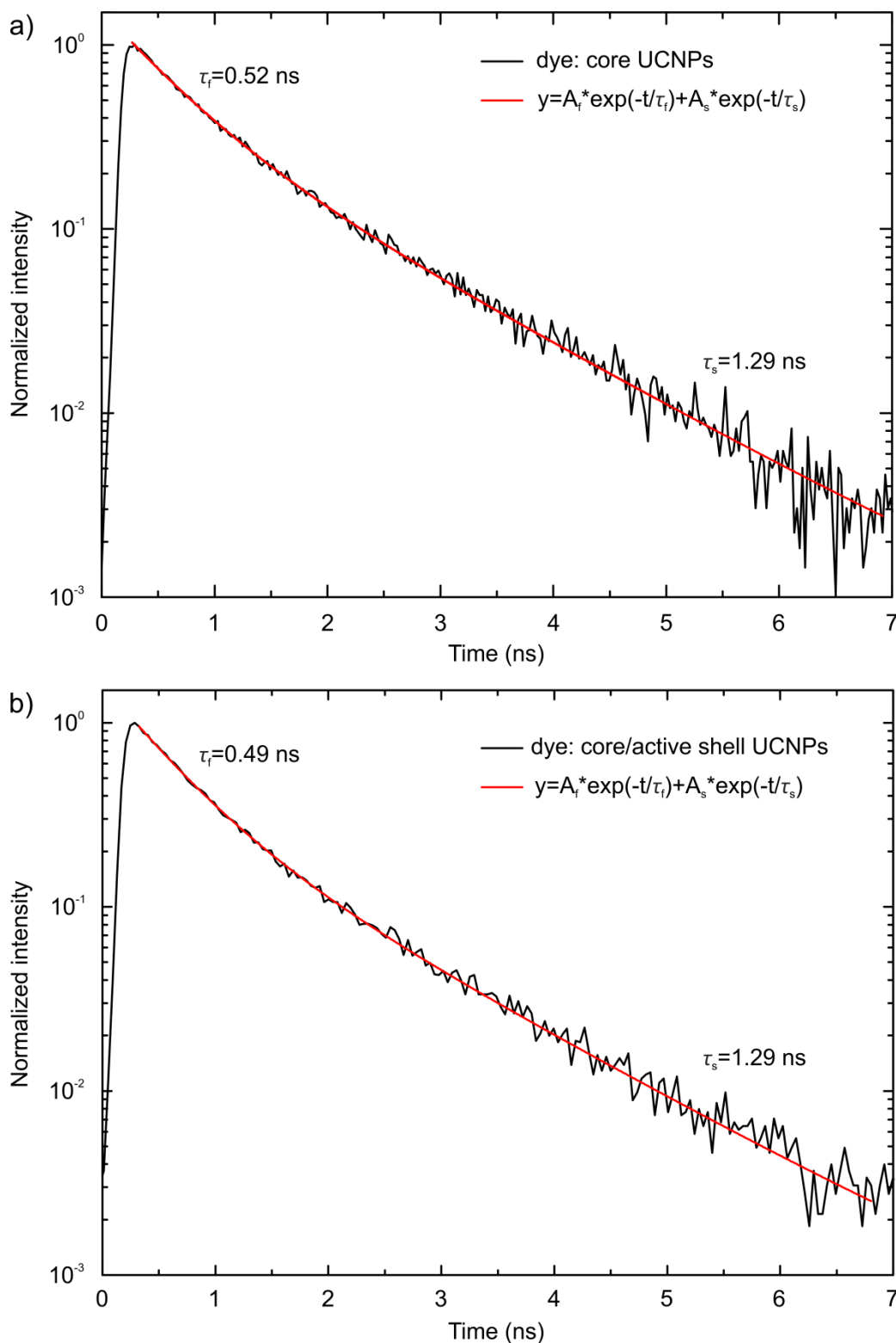


**Figure S1.** The fluorescence decay curves of the dye IR-806 molecules (black solid curves) attached to the surface of UCNPs pumped at 800 nm (1  $\mu$ W, 20 MHz) for a) core-only and b) core/active shell structure. Red solid curves show the results of bi-exponential fitting of the decay curves. The fitting error is less than 0.01 ns in both cases.

The amplitudes  $A_f$  and  $A_s$  of decay components are proportional to the relative concentration of bound and free dye respectively. As we described in the manuscript, the ratio of the amplitudes of the fast over the slow component of decay is  $A_f/A_s=2.76$  for core/active shell solution and  $A_f/A_s=1.99$  for core-only UCNPs solution. This leads to reasonable evaluation of free dye fraction in solutions as  $100\% / (1+2.76)\approx 26.6\%$  for dye-sensitized core/active shell UCNPs solution, and  $100\% / (1+1.99)\approx 33.3\%$  for dye-sensitized core-only UCNPs solution. Therefore, approximately 73.4% of all dye molecules are bound with core/active shell UCNPs and 66.7% of dye are bound with core-only UCNPs. This difference can be explained by different surface area of core-only and core/active shell UCNPs.

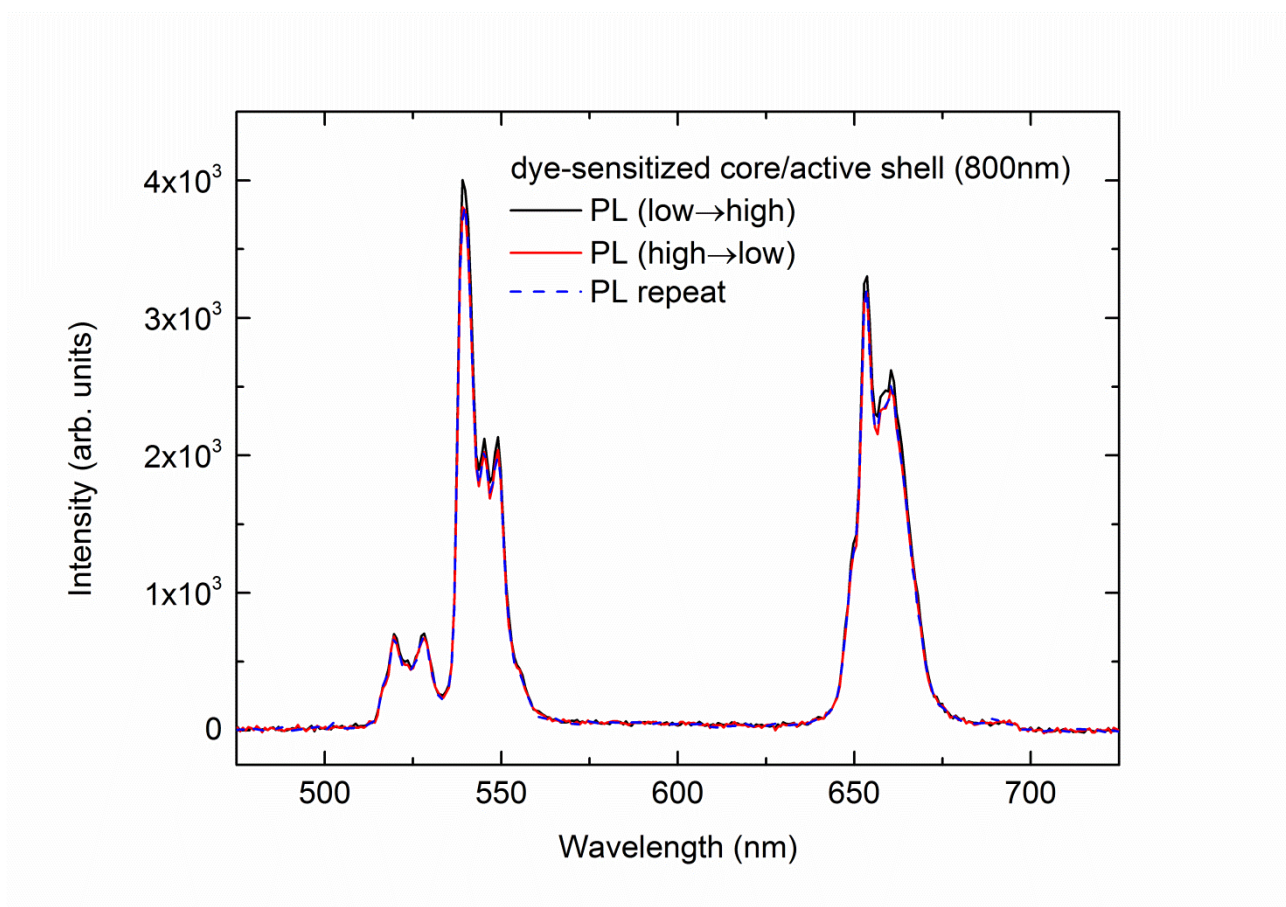


**Figure S2.** Reproducibility of upconversion luminescence signal (at 800 nm photoexcitation) to demonstrate short-term photostability of dye-sensitized UCNPs. Black solid curve shows

photoluminescence (PL) of UCNPs when excitation power (here 50  $\mu\text{W}$ ) was increased step by step from low value (8  $\mu\text{W}$ ) to higher (75  $\mu\text{W}$ ). Red curve shows PL of UCNPs when excitation power was decreased from 75  $\mu\text{W}$  to 50  $\mu\text{W}$ . Blue dashed curve shows results of repeated one more time PL measurement at 50  $\mu\text{W}$  excitation.

During all measurements the quartz cuvette with solution was sealed and continuously scanned in focal plane of the focusing microscope objective using an automated translation stage. This approach facilitates effective mixing of the solution while allowing for high reproducibility of the results due to ensemble averaging and reduces detrimental local heating. We investigated only short-term photostability ( $\sim 20$  min) of the IR-806 dye-sensitized UCNPs: after measurement of the power dependence starting from lower excitation value 8  $\mu\text{W}$  to higher 75  $\mu\text{W}$  we again decreased the intensity to lower value (50  $\mu\text{W}$ ) and observed perfect coincidence (see figure above). By utilizing the experimental methods described above we are confident that our results are reproducible and not affected by the photodegradation of the sample.

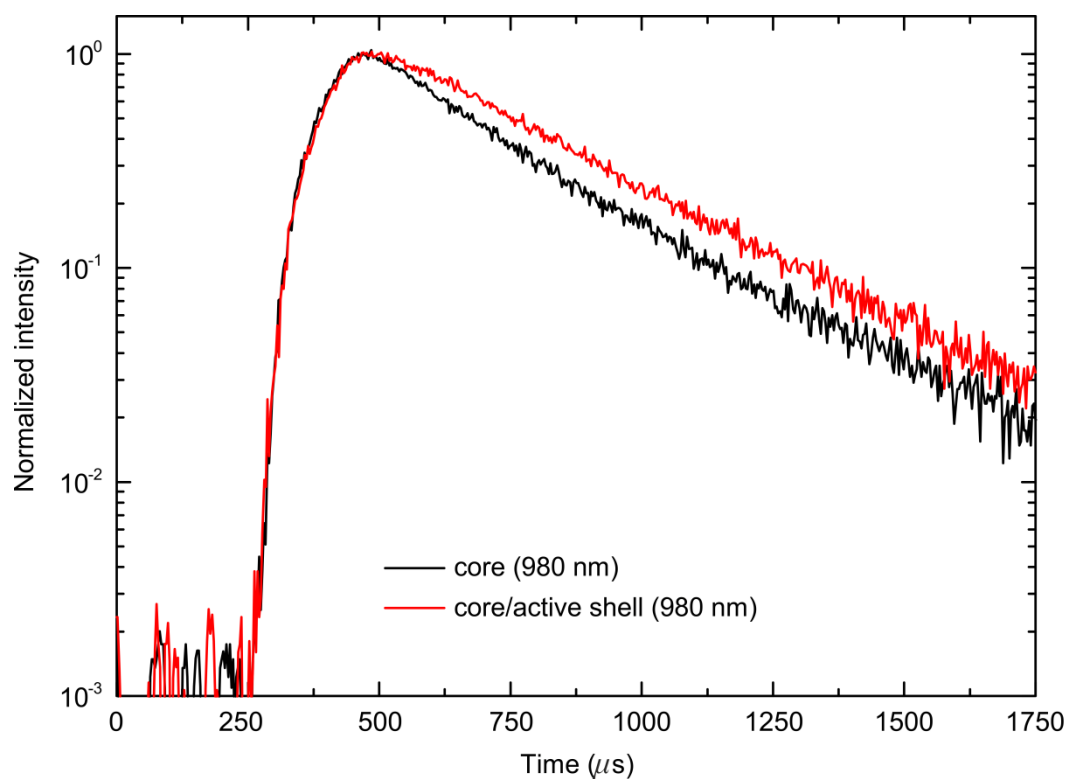


**Figure S3.** Upconversion kinetics of non-sensitized core-only (black solid curve) and core/active shell (red solid curve) UCNPs pumped at 980 nm with frequency of 295 Hz, duty cycle 5%. The rise dynamics of upconversion luminescence is identical, while the decay time is longer for core/active shell UCNPs.

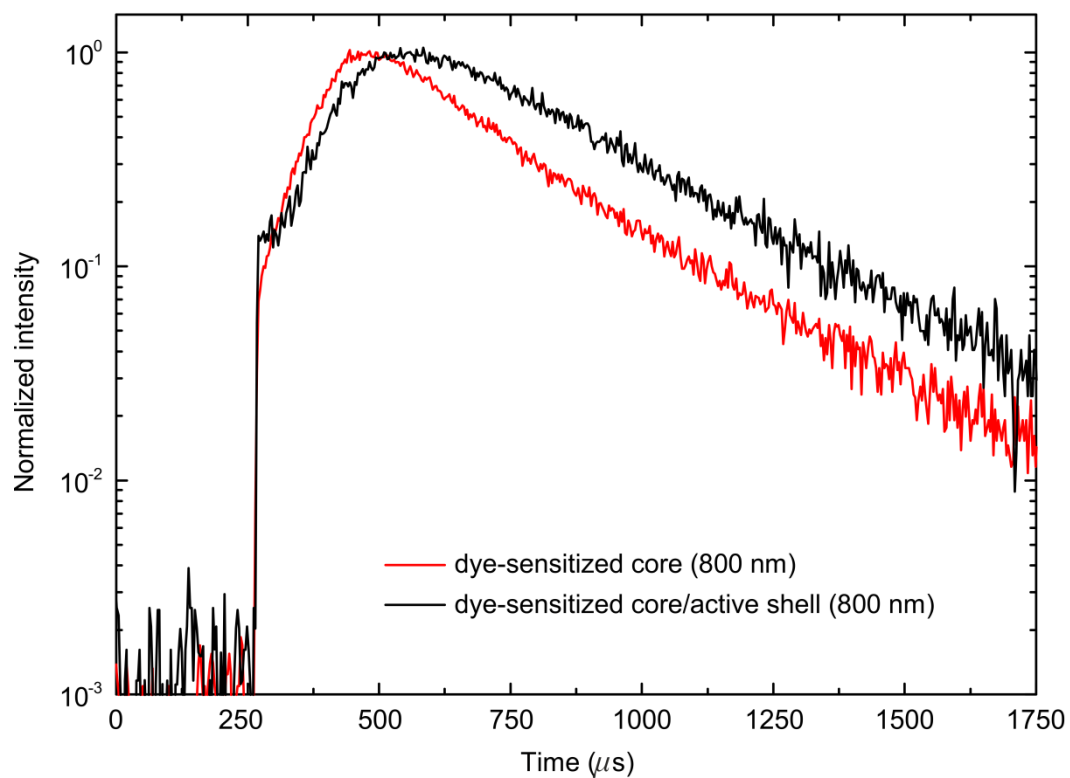


**Figure S4.** Upconversion kinetics of dye-sensitized core/active shell (black solid curve) and dye-sensitized core-only (red solid curve) UCNPs pumped at 800 nm with frequency of 295 Hz, duty cycle 5%.

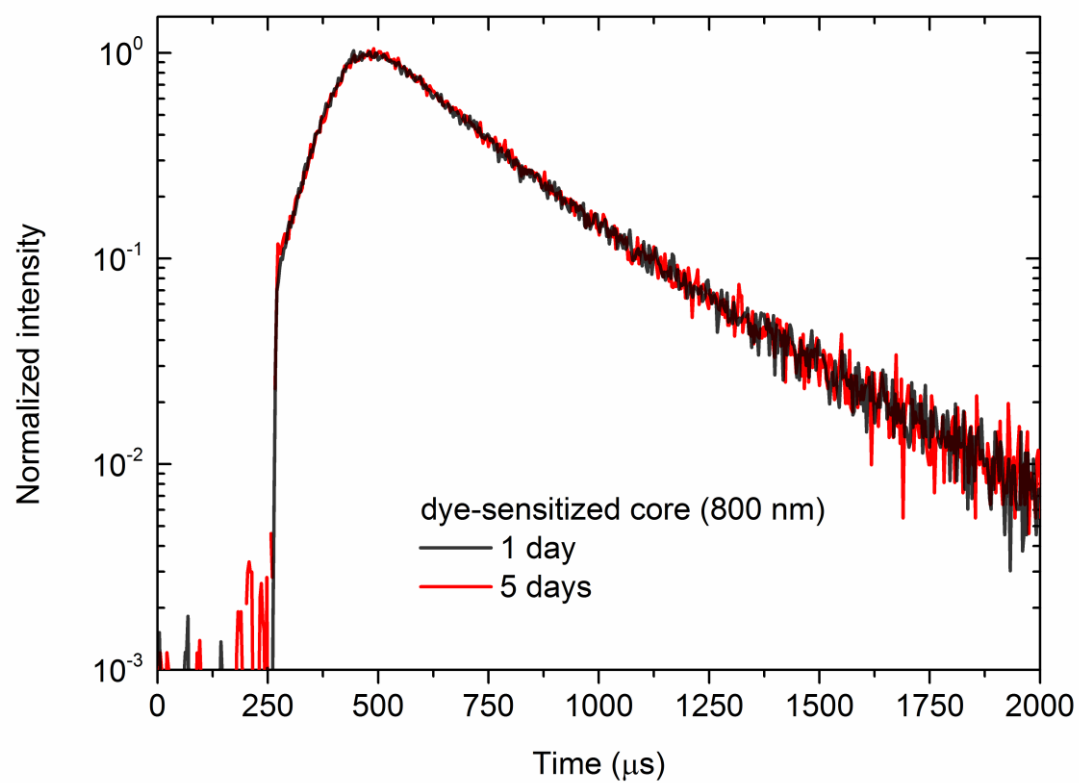


**Figure S5.** High reproducibility of upconversion luminescence kinetics after 5 days of storing sample in the fridge and full cycle of optical characterization. This figure reflects binding stability of the dye-sensitized UCNPs at least within 5 days.

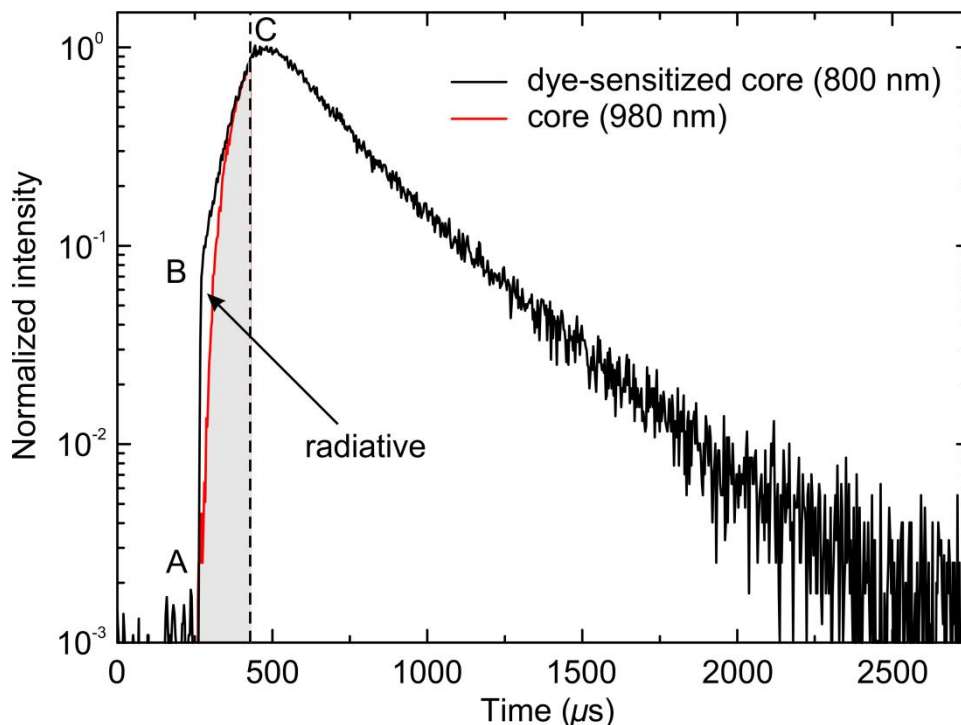


**Figure S6.** Evaluation of radiative channel efficiency. The difference in total area under the curves that correspond to upconversion kinetics of dye-sensitized core and core UCNPs reflects the contribution of radiative energy transfer. Dashed line shows termination of the excitation pulse ( $\approx 169 \mu\text{s}$ ). The excitation frequency (295 Hz) allows the excited states of  $\text{Er}^{3+}$  to decay completely before the next pulse train comes.

The non-radiative channel of energy transfer from excited  $\text{Yb}^{3+}$  to  $\text{Er}^{3+}$  is characterized by slow rise dynamics of upconversion kinetics (red solid curve) of core-only UCNPs. The slow component (BC) of kinetics of dye-sensitized core-only UCNPs at the moment of pulse termination coincides with red curve that describes non-radiative channel only. Consequently, total contribution of radiative energy transfer in dye-sensitized UCNPs can be estimated as difference of integrated area under the corresponding curves:

$$R = \int_0^{\tau} [I_{\text{dye-sens core}}(t) - I_{\text{core}}(t)] dt \quad (1)$$

Therefore, the relative contribution of radiative energy transfer –  $r$  equals:



$$r = \frac{R}{\int_0^T I_{dye-sens\ core}(t)dt} \quad (2)$$

where T – period of excitation. These formulae give  $r \approx \frac{60.7-52.5}{398} \approx 0.02$ . This means that the non-radiative channel of energy transfer is major channel of energy transfer, while radiative component gives just about 2% of detected photons under pulsed excitation. The estimation of radiative channel contribution in luminescence rise dynamics (up to the moment of PL maximum) gives  $10 \pm 1$  %.

The optimum dye concentration was found to be equal for dye-sensitized core and core/active shell UCNP's solution. This means equal total number of dye molecules in both solutions. We note that radiative energy transfer from dye to UCNP's can occur either from free dye or from dye attached to the surface of UCNP. However, the density of dye at surface of UCNP is higher than that in ambient solution. We calculate below the relative efficiency of radiative channel for dye that can transfer energy to core-only and core/active shell UCNP's. This parameter determines the proportion of energy that is relaxed through photons emission. This value equals:

$$R = \frac{K_R^0}{K_{TOTAL}} = \frac{QY * K_{TOTAL}^0}{K_{TOTAL}} = \frac{QY * (1/\tau_0)}{1/\tau} = QY \frac{\tau}{\tau_0} \quad (3)$$

Where QY – quantum yield of the free dye,  $\tau$  – lifetime of dye bound to surface of UCNP's,  $\tau_0$  – lifetime of free dye in solution,  $K_R^0$  – rate of radiative relaxation for free dye,  $K_{TOTAL} = (K_{TOTAL}^0 + K_{NR})$  - total rate of relaxation for the dye bound to UCNP's. Therefore, for the dye bound to core/active shell and core-only UCNP's ratio of the R coefficients is given by:

$$\frac{R_{core-act\ sh}}{R_{core}} = \frac{QY * \frac{\tau_{core-act\ sh}}{\tau_0}}{QY * \frac{\tau_{core}}{\tau_0}} = \frac{\tau_{core-act\ sh}}{\tau_{core}} = \frac{0.49\ ns}{0.52\ ns} \approx 0.94 \quad (4)$$

**Table S1.** The main parameters used for estimation.

Solution	Fraction of bound dye	Non-radiative ET efficiency	Size of UCNPs	Size of core
Core UCNPs	66.7%	59.7%	32.9 nm	32.9 nm
Core/active shell UCNPs	73.4%	62%	39.7 nm	31.2 nm

The total energy absorbed by Er ions inside the core of the nanoparticles due to radiative photon energy transfer by the dye molecules attached to the surface of nanoparticle is proportional to efficiency of the radiative channel for dye, the absorption-cross section of dye at 800 nm, the absorption cross-section of Er at  $\approx 980$  nm, the fraction of bound dye molecules, the number of Er ions (proportional to volume of the core) and the surface area of the nanoparticles. Therefore, the ratio of the total energy absorbed by Er ions in core and core/active shell UCNPs due to direct absorption of the dye emission equals:

$$\frac{E_{core-act\ shell}}{E_{core}} \approx 0.94 * \frac{73.4}{66.7} * \left(\frac{31.2}{32.9}\right)^3 \left(\frac{39.7}{32.9}\right)^2 \approx 1.28 \quad (5)$$

Since upconversion is a nonlinear process, the ratio of detected UCL intensities due to radiative energy transfer is  $\sim (1.28)^2 \approx 1.64$ . This value perfectly coincides with ratio of amplitudes of the fast components in the rise dynamics of upconversion luminescence  $(0.137 \pm 0.002)/(0.085 \pm 0.002) \approx 1.61$ , (mind log scale) that we attributed in the manuscript to radiative energy transfer from dye to Er. We believe that the agreement we obtain from the analysis of our experimental results on the upconversion kinetics provides strong evidence of the fair-minded conclusions drawn in the manuscript.

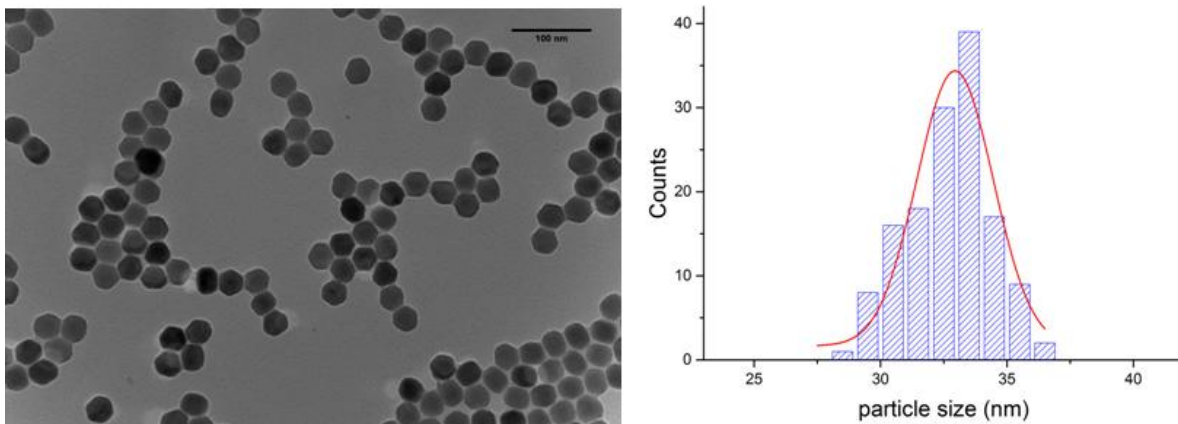


**Figure S7.** TEM image (left) and corresponding size distribution (right) of core  $\beta$ -NaYF<sub>4</sub>:Yb<sup>3+</sup>(20%),Er<sup>3+</sup>(2%) UCNPs with a size  $32.9 \pm 1.6$  nm. Scale bar 100 nm.

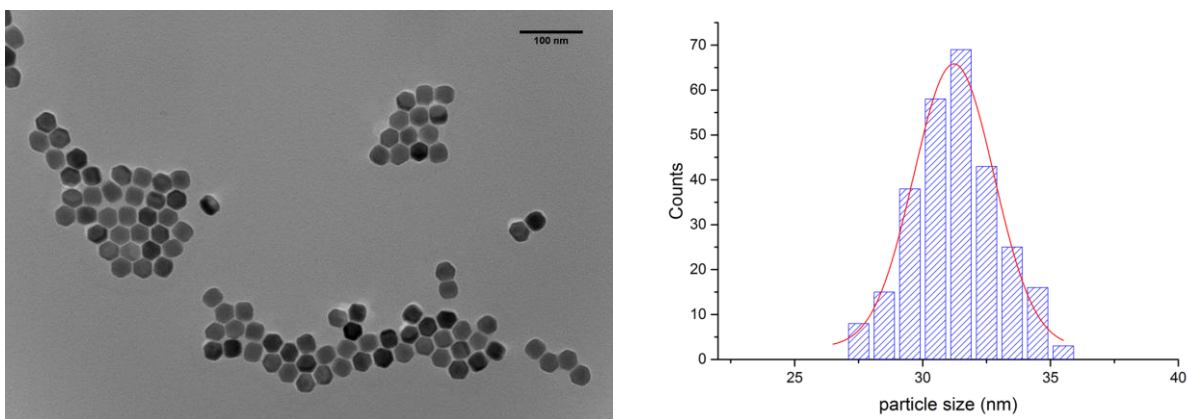


**Figure S8.** TEM image (left) and corresponding size distribution (right) of core  $\beta$ -NaYF<sub>4</sub>:Yb<sup>3+</sup>(20%),Er<sup>3+</sup>(2%) UCNPs with a size  $31.2 \pm 1.6$  nm used to create the core/active shell UCNPs. Scale bar 100 nm.

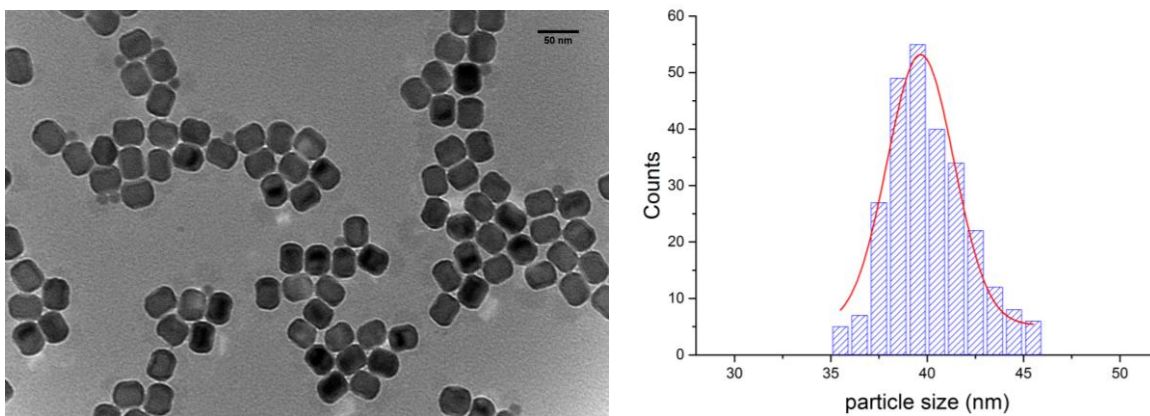


**Figure S9.** TEM image (left) and corresponding size distribution (right) of core/active shell  $\beta$ -NaYF<sub>4</sub>:Yb<sup>3+</sup>(20%),Er<sup>3+</sup>(2%)@NaYF<sub>4</sub>:Yb<sup>3+</sup>(10%) with a size of  $39.7 \pm 1.7$  nm. Scale bar 50 nm.

As reported in the literature<sup>1</sup> the small nanoparticles (~10 nm) observed on the TEM image in Figure S9 are byproducts of the synthesis. They are composed of NaYF<sub>4</sub>:Yb<sup>3+</sup> and do not possess any optical signature, therefore they do not contribute in our experimental observations.

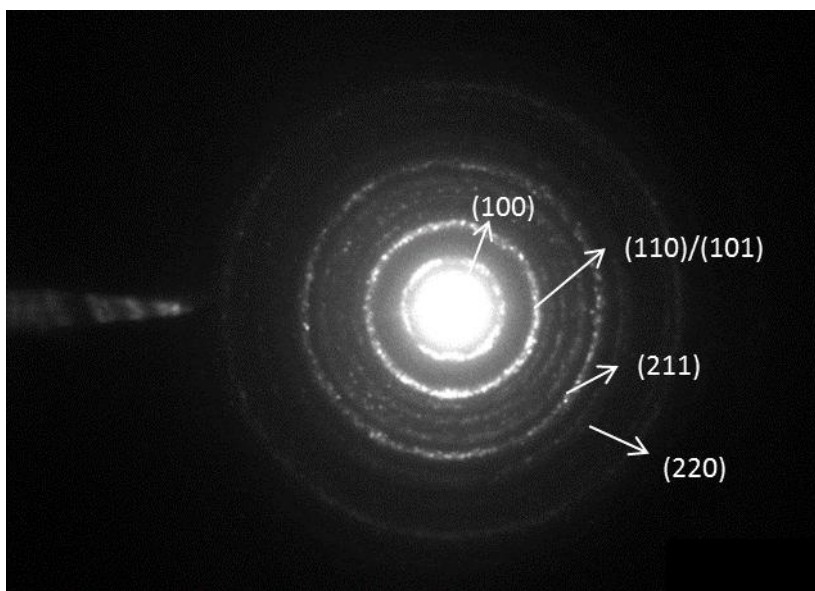


**Figure S10.** SAED pattern indicating a hexagonal phase of the core UCNP.

CHEMICAL FUNCTIONALIZATION AND CHARACTERIZATION OF THE NEAR IR  
DYE.

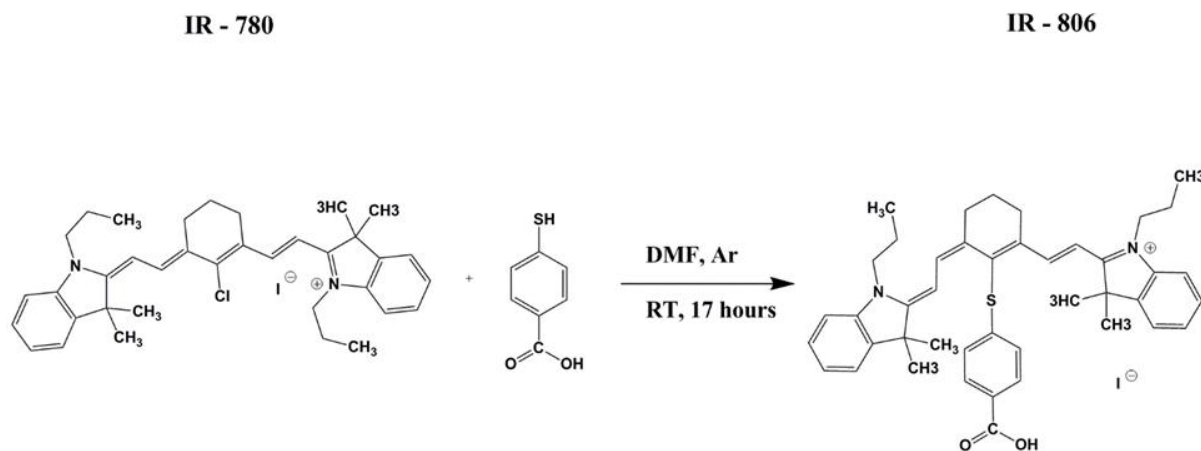


**Figure S11.** Synthesis of IR-806 showing a nucleophilic substitution of the central chlorine atom in IR-780 which is used to prepare the carboxylic acid derivated IR-806.

**Peak 1, RT 2.615, Scan 746, NL 1.194E08, MS2 (150:1500) ES+**

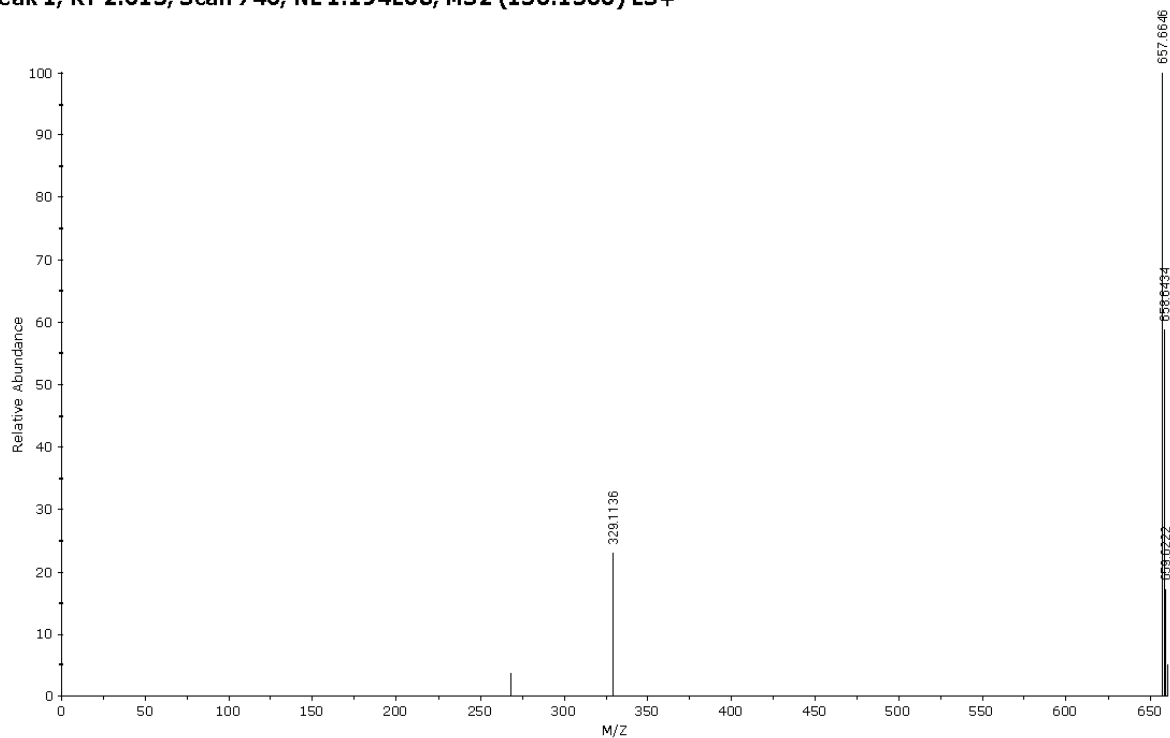


**Figure S12.** HRMS spectrum of IR-806 (experimental). HRMS: calculated for  $C_{43}H_{49}N_2O_2S$   $[M]^+ = 657.35$ ;  $[M]^+ = 657.66$  found.

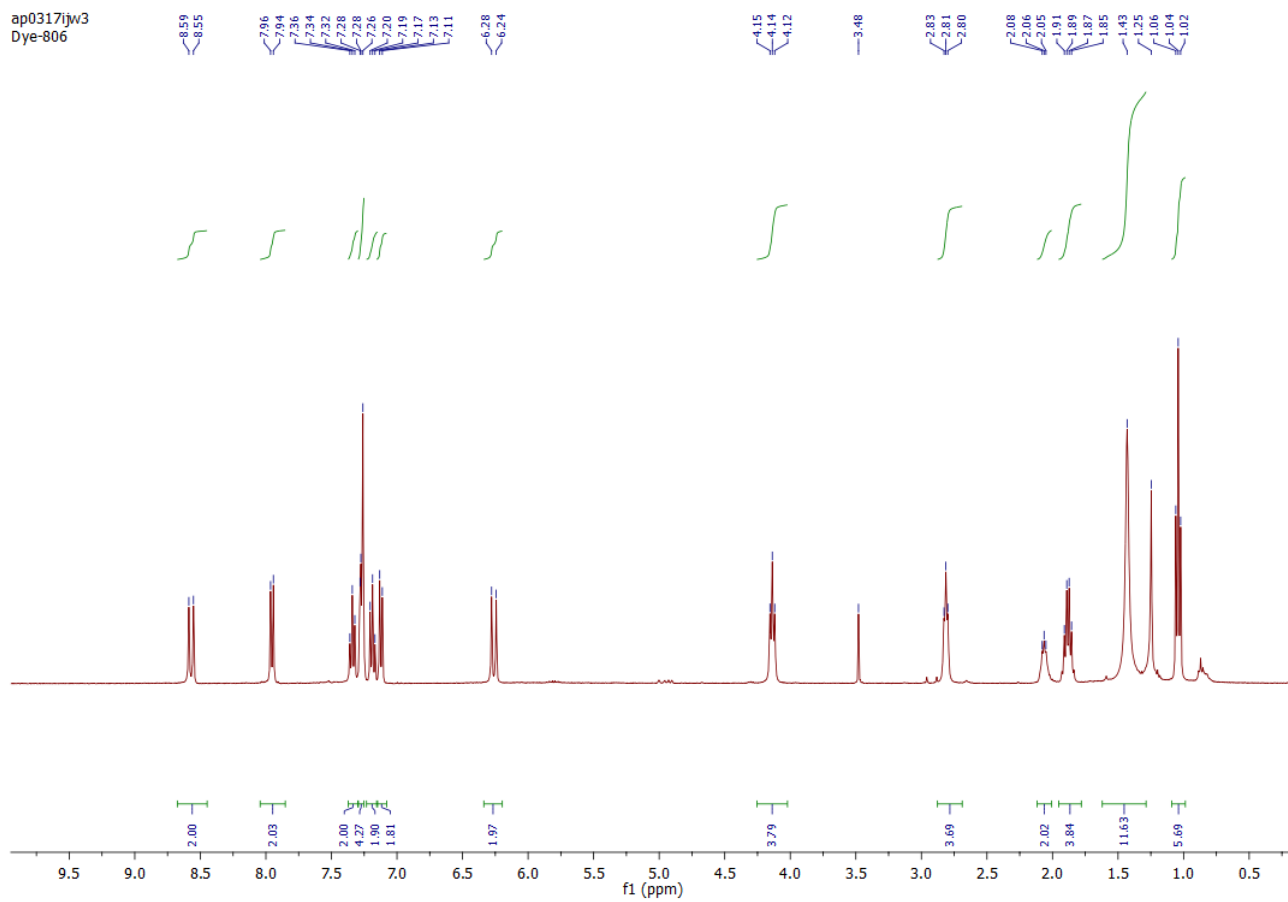


**Figure S13.**  $^1\text{H}$ -NMR (400 MHz,  $\text{CDCl}_3$ ), spectrum of IR-806.  $^1\text{H}$  NMR (400 MHz,  $\text{CDCl}_3$ ):  $\delta$  8.57 (d,  $J = 14.1$  Hz, 2H), 7.95 (d,  $J = 8.5$  Hz, 2H), 7.34 (t,  $J = 7.6$  Hz, 2H), 7.30 – 7.23 (m, 6H), 7.19 (t,  $J = 7.4$  Hz, 2H), 7.12 (d,  $J = 8.0$  Hz, 2H), 6.26 (d,  $J = 14.1$  Hz, 2H), 4.14 (t,  $J = 7.2$  Hz, 4H), 2.81 (t,  $J = 5.7$  Hz, 4H), 2.11 – 2.01 (m, 2H), 1.87 (dd,  $J = 14.6$  Hz,  $J = 7.3$  Hz, 4H), 1.43 (s, 12H), 1.04 (t,  $J = 7.4$  Hz, 6H).

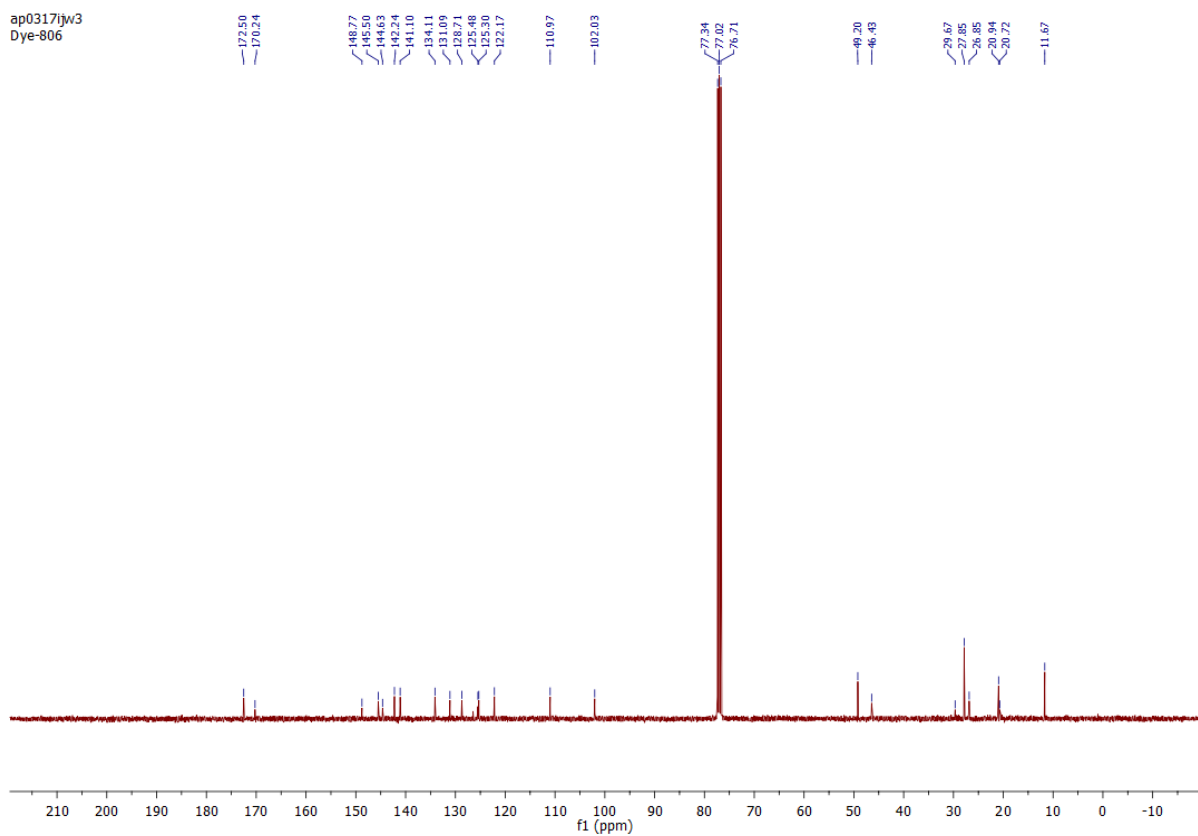


**Figure S14.**  $^{13}\text{C}$ - NMR (101MHz,  $\text{CDCl}_3$ ) spectrum of IR-806.  $^{13}\text{C}$  NMR (101 MHz,  $\text{CDCl}_3$ ):  $\delta$  172.52, 170.26, 148.79, 145.52, 144.65, 142.26, 141.12, 134.13, 131.11, 128.73, 125.50, 125.32, 122.19, 110.99, 102.05, 49.22, 46.45, 29.69, 27.87, 26.87, 20.96, 20.74, 11.69.

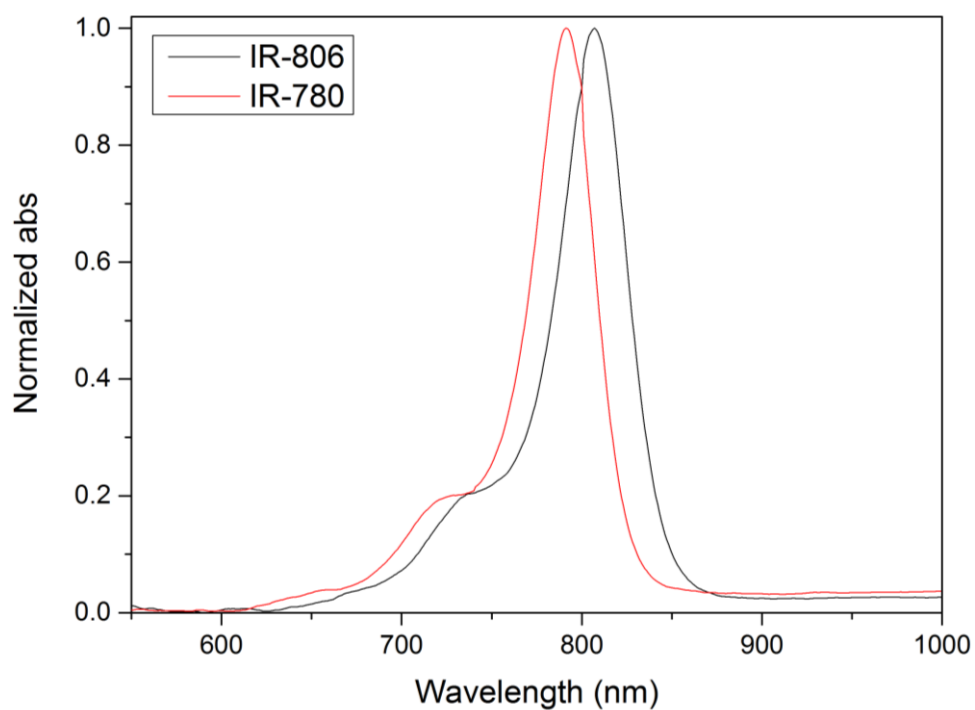


**Figure S15.** Normalized absorption spectrum of IR-806 and IR-780.

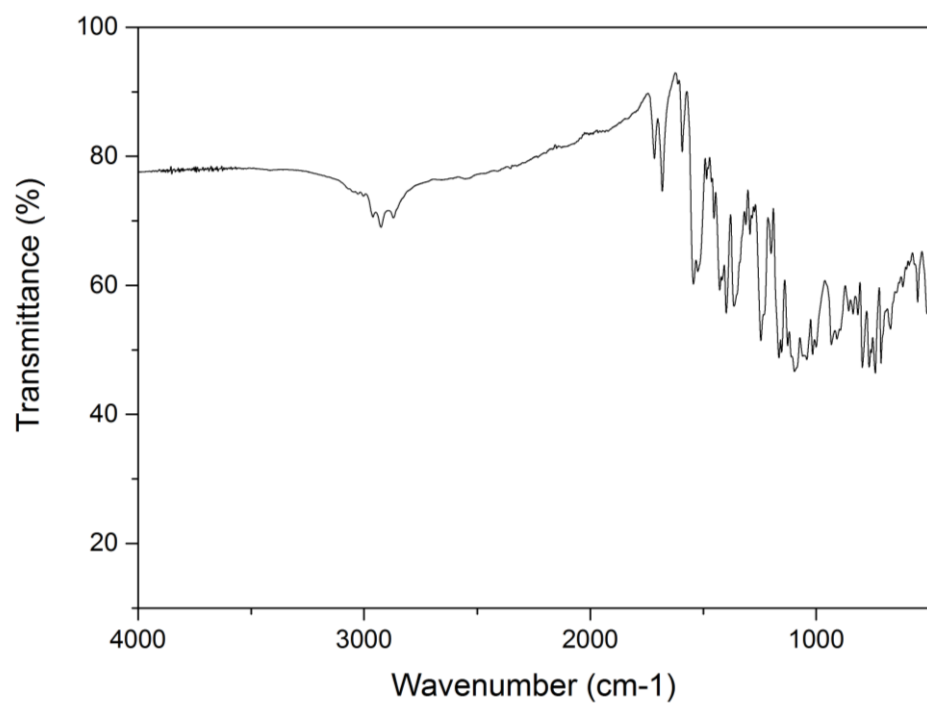


**Figure S16.** FT-IR spectrum of IR-806.



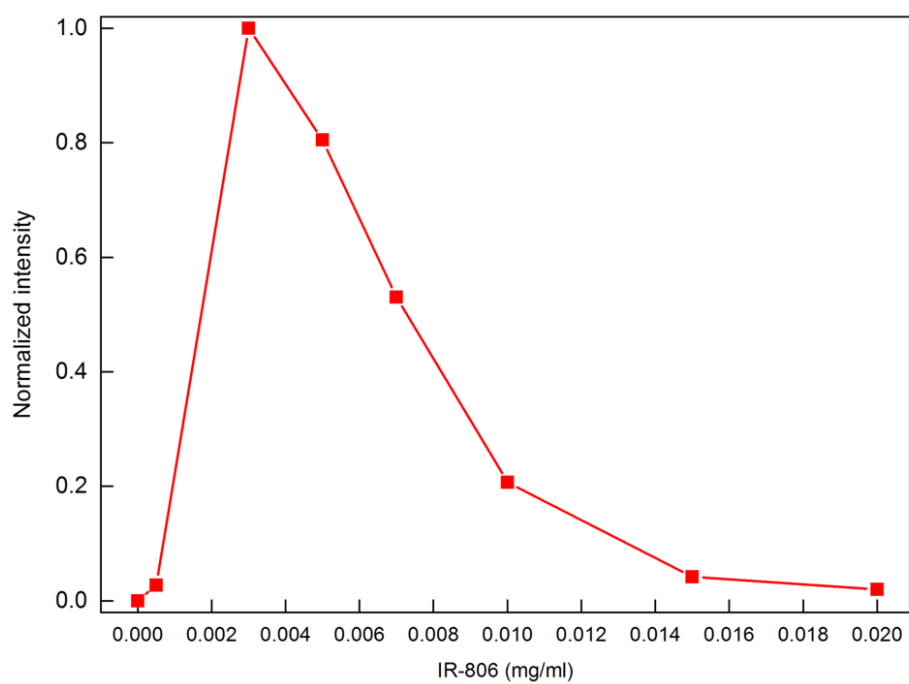


**Figure S17.** Integrated in spectral range of 500-690 nm upconversion luminescence intensity of core  $\beta$ -NaYF<sub>4</sub>:Yb<sup>3+</sup>(20%),Er<sup>3+</sup>(2%) UCNP (0.8mg/ml) as a function of IR-806 content in CHCl<sub>3</sub> excited by 2mW 800 nm laser.

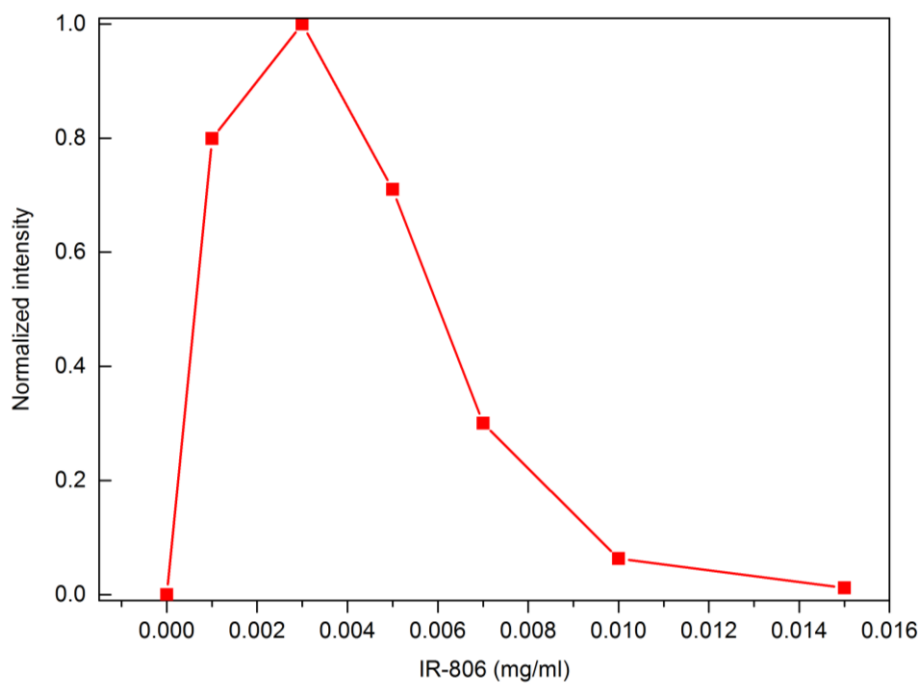


**Figure S18.** Integrated in spectral range of 500-690 nm upconversion luminescence intensity of core/active shell UCNPs (the core UCNPs that were used to create the core/active shell UCNPs were 0.8mg/ml) as a function of IR-806 content in  $\text{CHCl}_3$  excited by 2mW 800 nm laser.

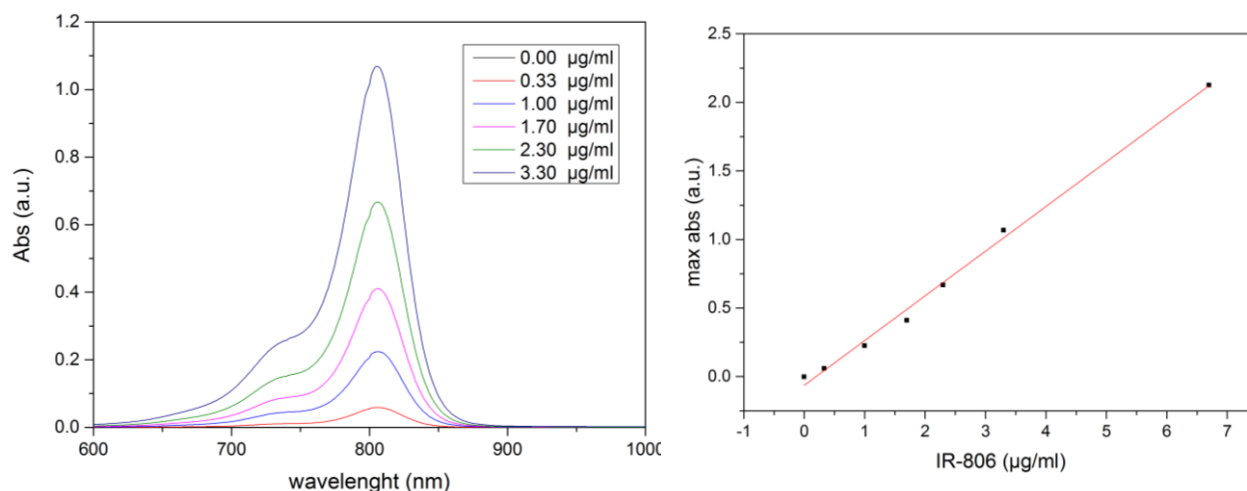


**Table S2.**

Solution	$C_0$ ( $\mu\text{g/ml}$ )	$C_1$ ( $\mu\text{g/ml}$ )	Fraction of bound dye	Fraction of dye free in solution
Core UCNPs	$0.34 \pm 0.01$	$2.66 \pm 0.03$	$88.6\% \pm 1.9\%$	$11.3\% \pm 0.3 \%$
Core/active shell UCNPs	$0.26 \pm 0.01$	$2.74 \pm 0.03$	$91.2\% \pm 1.9\%$	$8.8 \% \pm 0.3 \%$



**Figure S19.** Experimental estimation of the concentration of the free dye in solution. The solution containing the dye-coated core or core/active shell UCNPs was centrifuged at 10000 rpm 15 min to

extract the nanoparticles. Then the fluorescence signature of the dye was measured in the supernatants and the concentration of the free dye was calculated through a calibration curve.

Solutions were illuminated under a 980 nm laser pointer before and after the centrifugation to visualize the full precipitation of the nanoparticles. One can see that the green emission disappeared due the absence of the UCNPs in the collected supernatant. Furthermore, the absence of UCNPs in the supernatant was evaluated by absorbance spectroscopy. The linear portion of the calibration curve is fit with a line,  $y=0.3262x-0.06404$ .  $C_0$  is the concentration measured from supernatants and  $C_1$  is the concentration of the estimated Dye attached to the UCNPs. After measuring the supernatant concentrations we calculated that the fraction of the dye attached to the core is 88.6% and to the core-shell 91.2%.

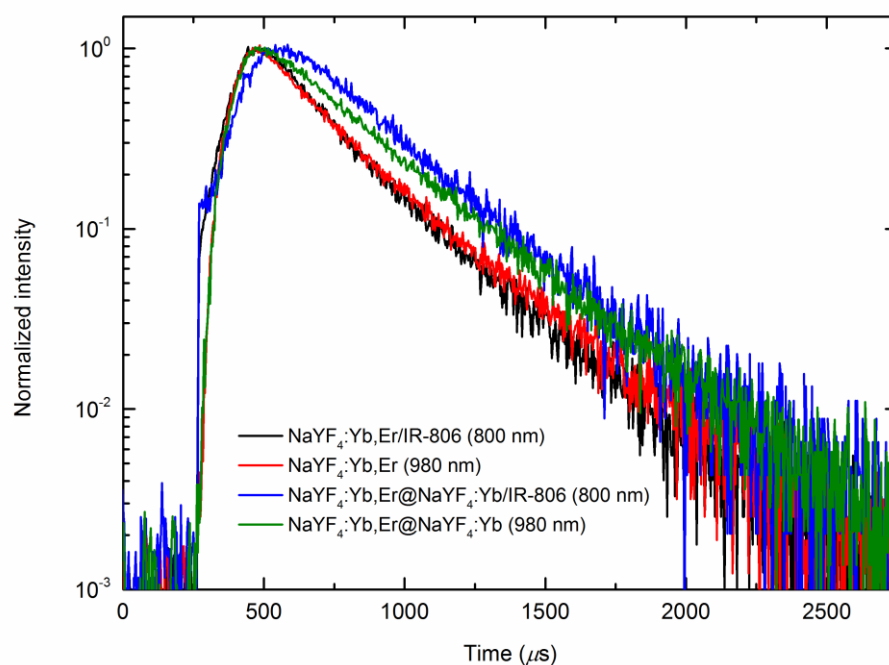


**Figure S20.** Upconversion kinetics of non-sensitized and dye-sensitized UCNPs pumped with 50  $\mu\text{W}$  at 980 nm and 800 nm, respectively for core and core/active shell structures, to demonstrate complete decay of excited states of  $\text{Er}^{3+}$  ions under the excitation at frequency of 295 Hz.

#### References:

- (1) Jiang, G.; Pichaandi, J.; Johnson, N. J. J.; Burke, R. D.; Van Veggel, F. C. J. M. An Effective Polymer Cross-Linking Strategy to Obtain Stable Dispersions of Upconverting  $\text{NaYF}_4$  nanoparticles in Buffers and Biological Growth Media for Biolabeling Applications. *Langmuir* **2012**, 28 (6), 3239-3247